Organic Electronics 13 (2012) 31–35

Contents lists available at SciVerse ScienceDirect

Organic Electronics

journal homepage: www.elsevier.com/locate/orgel

Full color organic electroluminescent display with shared blue light-emitting layer for reducing one fine metal shadow mask

Shuming Chen, Hoi-Sing Kwok *

Center for Display Research, Department of Electronic and Computer Engineering, The Hong Kong University of Science and Technology, Clear Water Bay, Kowloon, Hong Kong

ARTICLE INFO

Article history:
Received 12 July 2011
Received in revised form 23 September 2011
Accepted 1 October 2011
Available online 18 October 2011

Keywords:
Organic electroluminescent display
Find metal shadow mask
Full color
Manufacturing cost

ABSTRACT

To make a full color organic electroluminescent display, conventionally it requires three fine metal shadow masks (FMM) to pattern the red, green and blue light-emitting layer. In this work, by arranging the blue light-emitting layer as a shared layer for all sub-pixels, we demonstrate that a full color display can be achieved by two FMM processes, thus reducing one FMM process compared to conventional method. The red, green and blue sub-pixels can be optimized independently despite the reduction of one FMM process. Also, the performance of the red and green sub-pixels is not degraded by the shared blue light-emitting layer. Due to elimination of one FMM, the process TACT time, mask cost and alignment error can all be reduced, thus cutting down the manufacturing cost of full color organic electroluminescent display.

1. Introduction

Organic electroluminescent display (or organic light-emitting display, OLED) featuring wide range of working temperature, low power consumption, wide viewing angle, fast response time, high contrast and vivid color are very attractive for next generation flat-panel-display applications [1–8]. A typical OLED pixel consists of two or more organic layers sandwiched between a transparent indium–tin-oxide (ITO) anode and a reflective metallic cathode. A full color pixel in general consists of three sub-pixels which emit three primary colors red (R), green (G) and blue (B). The sub-pixel can be patterned by a find metal shadow mask (FMM) with many tiny openings. Through the openings, organic light-emitting materials are deposited and defined onto the substrate. The FMM typically is made by electroforming or etching the stainless steel, which can generate an opening as small as 50 μm [1]. The FMM has some intrinsic limitations such as expensive, thermal expansion, mechanical bending and difficult handling when the size is increased, rendering it unsuitable for large area and high resolution display applications [1–3]. To circumvent this problem, alternative color patterning schemes are proposed like inkjet printing of soluble OLED materials [4,5], laser-induced thermal transferring of organic materials [6,7], and combination of unpatterned white OLED with photolithography patterned color filter [3,8], etc. However, all of them are still in their developing phase and not ready for commercial production. Till now, FMM is still the most mature and successful method for commercial production despite its intrinsic shortcomings.

The FMM is aligned to a substrate by a high precision mechanism. As shown in Fig. 1, there are two alignment methods namely active and passive alignment. In an active approach [9], CCD cameras are used to capture the alignment marks of the substrate and FMM. The relative

Abbreviations: BCzVBi, 4,4′-bis(9-ethyl-3-carbazovinylene)-1,1′-biphenyl; FIrPic, bis(3,5-difluoro-2-(2-pyridyl)phenyl)-(2-carboxypyridyl)iridium(III); $Ir(btp)_2(acac)$, bis(2-benzo[b]thiophen-2-yl-pyridine)(acetylacetonate)iridium(III); $Ir(ppy)_3$, fac-tris(2-phenylpyridine)iridium(III); CBP, 4,4′-bis(carbazol-9-yl)biphenyl; NPB, *N*,*N*′-bis(naphthalen-1-yl)-*N*,*N*′-bis(phenyl)-benzidine; TPBi, 2,2′,2″-(1,3,5-benzinetriyl)-tris(1-phenyl-1-H-benzimidazole); TcTa, 4,4′,4″-tris(carbazol-9-yl)triphenylamine.

* Corresponding author.
E-mail addresses: smchen@ust.hk (S. Chen), eekwok@ust.hk (H.-S. Kwok).

1566-1199/$ - see front matter © 2011 Elsevier B.V. All rights reserved.
doi:10.1016/j.orgel.2011.10.002

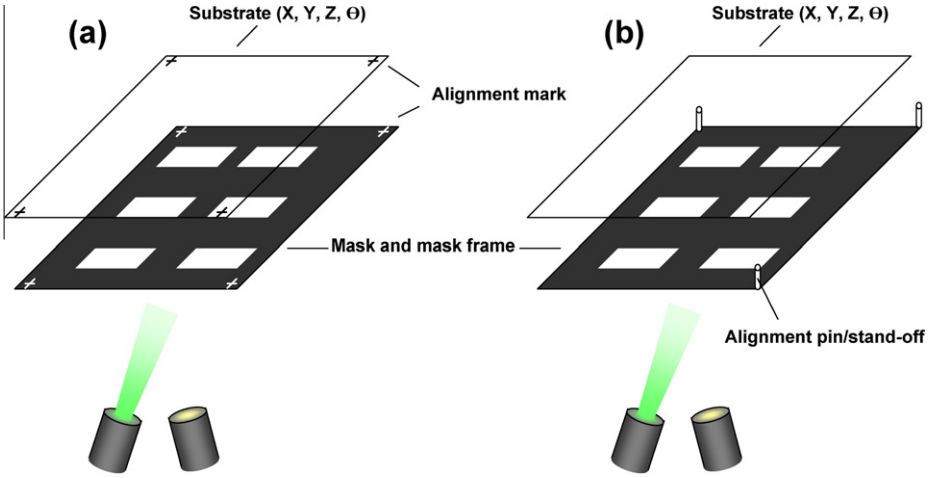

Fig. 1. Active (a) and passive (b) alignment method for aligning a shadow mask to a substrate. Due to precisely moving and adjusting of the substrate or mask, the alignment process tends to be slow.

position between the FMM and the substrate is then calculated by a computer. The mask or substrate is then reposition by a high precision motion system to reduce the alignment error. For a passive alignment [10–12], alignment pins or stand-off are placed on the mask frame, the edges of the substrate are then aligned to the FMM by placing them in contact with the pins, as shown in Fig. 1(b). Both alignment methods tend to be time consuming due to the precisely moving and adjusting of the substrate or mask. For a full color display, R, G and B sub-pixels with different emission area are generally adopted to reduce the differential aging of R, G and B sub-pixels [13]; thus one has to employ three different FMMs and perform three alignments for patterning the R, G and B sub-pixels, yielding a long process TACT time and expensive mask cost. To relieve this issue, Samsung and Sony proposed stacking a blue layer on the patterned G (and R) layer as a common layer for all sub-pixels, thus eliminating the patterning of the B sub-pixels [14,15]. To avoid exciton recombination in the common B layer in the G (or R) sub-pixels, a wide band-gap host with hole-blocking ability was adopted for the G (and R) dopants, which inevitably increases the

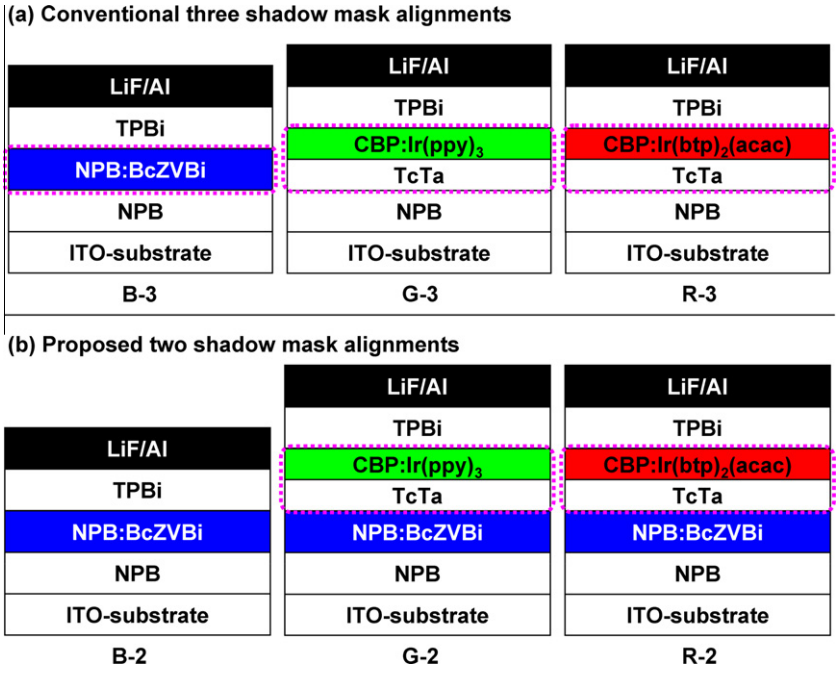

Fig. 2. Device structures of conventional three FMM processes (a) and proposed two FMM processes (b). The light-emitting layers need to be patterned are surrounded by a dot line.

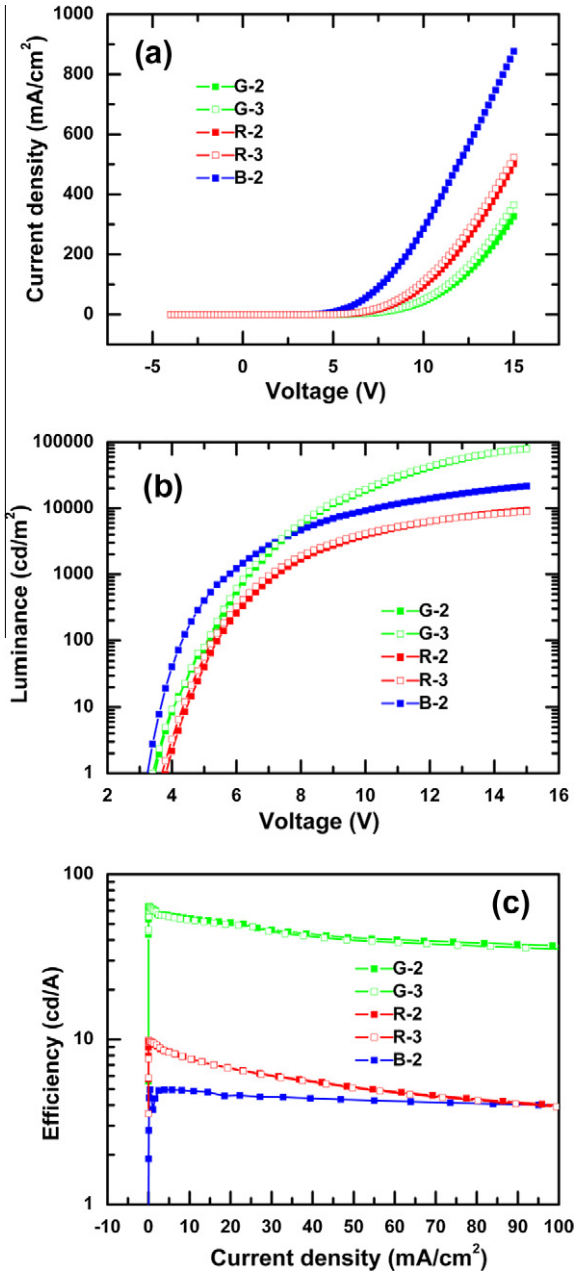

Fig. 3. Current density–voltage (a), luminance–voltage (b) and efficiency–current density (c) characteristics of the devices. The key characteristics of the devices made by two FMM processes are not degraded by the shared blue light-emitting layer.

driving voltage of the pixels; for example, at a luminance of 239 cd/m^2, the driving voltage is 6.5 V for the Ir(ppy)$_3$ based G pixels [14].

In this work, in order to avoid using wide band-gap host for the G (and R) dopants, we deposit the patterned G (and R) layer on the common B layer. In such configuration, the exciton main recombination zone is located in the interface of G/ETL due to the higher mobility of holes than that of electrons. Thanks to the narrower band-gap of the G (or R) emitter compared with that of the B emitter, the G (or R) emitter therefore naturally serves as a trap site for the carriers and thus self-confine the exciton recombining in the G (or R) layer, hence preventing excitons leakage to adjacent B common layer. With the B light-emitting layer as a shared hoe-transporting layer for all sub-pixels, we demonstrate that a full color display can be achieved by only patterning the R and G sub-pixels; thus eliminate one FMM process compared to conventional method. The R, G and B sub-pixels can be optimized independently despite the reduction of one FMM process. Also, the performance of the red and green sub-pixels is not degraded by the shared B light-emitting layer. Due to elimination of one FMM, the process TACT time, mask cost and alignment error can all be reduced, thus cutting down the manufacturing cost of full color OLED display.

2. Results and discussion

Fig. 2(a) shows the typical device structures for constructing a full color OLED display. Fluorescent B emitter BcZVBi was employed due to its relatively bluer emission than that of the phosphorescent emitter like FIrPic; while phosphorescent emitter Ir(ppy)$_3$ doped in CBP and Ir(btp)$_2$(acac) doped in CBP were employed as a G and R light-emitting layer respectively, due to their high efficiency and good color saturation. NPB and TPBi were employed as a shared hole-transporting and electron-transporting layer respectively for all sub-pixels. TcTa was used as an exciton-confining layer for the phosphorescent emitters. In conventional three FMM processes, the B light-emitting layer NPB:BcZVBi in sub-pixels B-3, G light-emitting layer TcTa/Ir(ppy)$_3$:CBP in sub-pixels G-3 and R light-emitting layer TcTa/Ir(btp)$_2$(acac):CBP in sub-pixels R-3 are patterned separately by three FMMs with different size openings. In the proposed two FMM processes as shown in Fig. 2(b), all sub-pixels share a blue light-emitting layer NPB:BcZVBi. For sub-pixels G-2 and R-2, the shared NPB:BcZVBi works as a hole-transporting layer, while for sub-pixels B-2, the NPB:BcZVBi functions as a B light-emitting layer. Thus the B FMM process is eliminated; one only need to pattern the TcTa/Ir(ppy)$_3$:CBP for sub-pixels G-2 and TcTa/Ir(btp)$_2$(acac):CBP for sub-pixels R-2.

There are several reasons for selecting the blue light-emitting layer NPB:BcZVBi as a shared layer. Firstly, the OLED behaves like a Fabry–Perot cavity [16,17], especially when the two electrodes are reflective as in top-emitting OLED. Cavity with thicker organic layers results in longer resonant wavelength. In other words, to optimize the emission efficiency, the B sub-pixels should have the thinnest organic layers while the R sub-pixels have the thickest organic layers. By arranging the B light-emitting layer as a shared layer, the cavity length of the B sub-pixels can be guaranteed the shortest while that of the G and R sub-pixels can be separately tuned by changing the thickness of G and R light-emitting layer respectively. Thus, one can still optimize the performance of the R, G and B sub-pixels independently despite the elimination of one FMM process. Secondly, the B emitter in general has the widest energy band-gap, which can be used to confine the excitons recombining in the G or R light-emitting layer. Hence, one may only observe monochromatic emission in the G-2

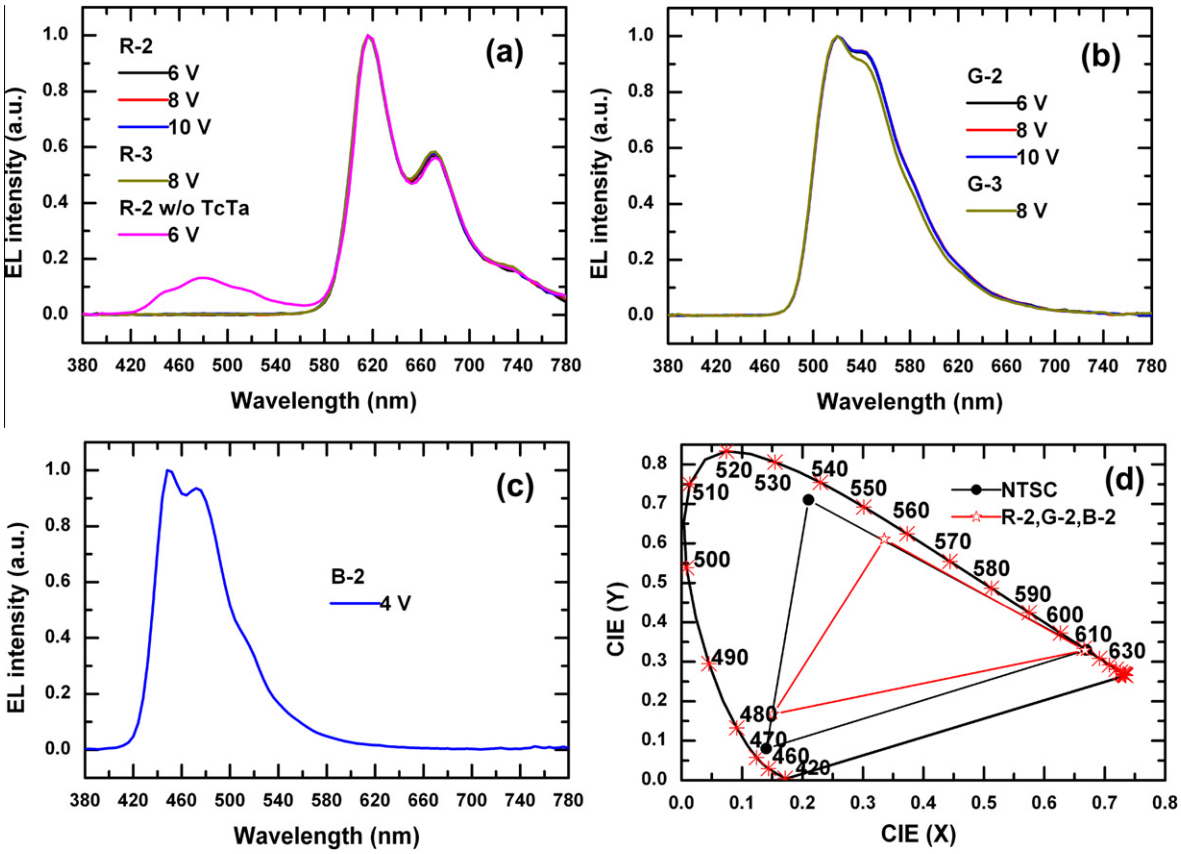

Fig. 4. EL spectra at different driving voltage of the R (a), G (b) and B (c) sub-pixels. Color gamut of the display made by two FMM processes (d).

Table 1
Key performance of the devices at 1000 cd/m^2.

Device	V (V)	η_{ext} (%)	η_L (cd/A)	η_P (lm/W)	CIE (x,y)
G-2	6.4	16.8	60.5	29.7	(0.34, 0.61)
G-3	6.4	16.6	59.5	29.2	(0.34, 0.61)
R-2	7.3	7.6	7.0	3.0	(0.67, 0.33)
R-3	7.2	7.6	7.0	3.1	(0.67, 0.33)
B-2	5.8	2.6	4.6	2.5	(0.15, 0.17)

or R-2 sub-pixels despite the presence of B light-emitting layer. Lastly, possible photoluminescent process of the shared layer excited by the G or R photons is completely eliminated due to extremely weak absorption of the B light-emitting layer at G or R color region.

To examine if the shared B light-emitting layer degrades the performance of the G-2 or R-2 sub-pixels, bottom emitting OLEDs were fabricated with structures:

G-2: ITO/NPB (20 nm)/8% BcZVBi:NPB (20 nm)/TcTa (10 nm)/8% Ir(ppy)$_3$:CBP (20 nm)/TPBi (40 nm)/LiF (1 nm)/Al (100 nm);
G-3: ITO/NPB (40 nm)/TcTa (10 nm)/8% Ir(ppy)$_3$:CBP (20 nm)/TPBi (40 nm)/LiF (1 nm)/Al (100 nm);
R-2: ITO/NPB (20 nm)/8% BcZVBi:NPB (20 nm)/TcTa (5 nm)/6% Ir(btp)$_2$(acac):CBP (20 nm)/TPBi (40 nm)/LiF (1 nm)/Al (100 nm);
R-3: ITO/NPB (40 nm)/TcTa (5 nm)/6% Ir(btp)$_2$(acac):CBP (20 nm)/TPBi (40 nm)/LiF (1 nm)/Al (100 nm);
B-2: ITO/NPB (20 nm)/8% BcZVBi:NPB (20 nm)/TPBi (40 nm)/LiF (1 nm)/Al (100 nm).

The fabrication and test method can be referred to our previous publications [18,19]. Fig. 3 shows the current density–voltage, luminance–voltage and efficiency–current density characteristics of the devices. It can be seen clearly that the introduction of the BcZVBi:NPB shared layer almost does not alter the characteristics of G-2 and R-2. Only a slightly decreasing of current density in devices G-2 and R-2 is observed, mainly caused by smaller mobility of NPB:BcZVBi than that of neat NPB. For example, at a driving voltage of 6.4 V, G-2 exhibit a current density of 1.67 mA/cm^2, luminance of 1014 cd/m^2 and efficiency of 60.5 cd/A, compared with 1.87 mA/cm^2, 1113 cd/m^2 and 59.5 cd/A for G-3. At a voltage of 7.2 V, R-2 exhibit a current density of 15.90 mA/cm^2, luminance of 1113 cd/m^2 and efficiency of 7 cd/A, compared with 15.99 mA/cm^2, 1124 cd/m^2 and 7.03 cd/A for R-3. The identical characteristics of G-2 and G-3, R-2 and R-3 indicate that all excitons may mainly recombine in the G or R light-emitting layer despite the presence of the B emitter BcZVBi. This may be likely due to the wide energy band-gap of BcZVBi and the introduction of exciton-confining layer TcTa, which effectively confine the excitons recombining in the G or R emitting layer.

To verify this assertion, the electroluminescent (EL) spectra of the devices are examined. As can be seen from Fig. 4(a) and (b), the EL spectra of G-2 and R-2 at 6–10 V are almost the same as those of G-3 and R-3, confirming that all excitons recombine in the G or R emitting layer despite the presence of B emitting layer in devices G-2 and R-2. Such excellent exciton confinement is likely due to the introduction of TcTa. Without the TcTa exciton-confining layer, a blue emission originates from BcZVBi is observed as shown in Fig. 4(a). It is well known that the triplet excitons have long life time thus long diffuse length. They tend to diffuse to adjacent layer, leading to exciton leakage hence efficiency loss. It is therefore necessary to introduce a thin layer of TcTa with high triplet energy level [20] and extremely low electron mobility [21] to effectively prevent excitons leakage to adjacent shared layer NPB:BcZVBi. Fig. 4(d) shows the CIE coordinates of devices R-2, G-2 and B-2. The color gamut of the display based on R-2, G-2 and B-2 is 63% NTSC. The low color gamut is mainly due to the unsaturated color of the G and B emission. To further improve the color gamut, microcavity structure may be employed to obtain narrower spectra hence saturated color [22]. The key performance of the devices is listed in Table 1.

3. Summary

In summary, we demonstrate that a full color OLED display can be achieved by two FMM processes. The reduction of one FMM compared with conventional three FMM processes is due to the adoption of a shared B light-emitting layer. The R, G and B sub-pixels can be optimized independently despite the elimination of one FMM process. Also, key characteristics like driving voltage, luminance, efficiency and spectra are not degraded by the shared blue light-emitting layer. Due to reduction of one FMM, the process TACT time, mask cost and alignment error can all be reduced, thus cutting down the manufacturing cost of full color OLED display.

Acknowledgment

This work was supported by the Hong Kong Government Research Grants Council Grant Nos. 614410 and AOE/P0308PG2.

References

[1] J.-J. Lih, C.-I. Chao, C.-C. Lee, Novel pixel design for high-resolution AMOLED displays with a shadow mask, J. Soc. Inf. Display 15 (2007) 3–7.
[2] H.D. Kim, J.K. Jeong, H.-J. Chung, Y.-G. Mo, Technological challenges for large-size AMOLED display, SID Int. Symp. Dig. Tech. Papers 39 (2008) 291–294.
[3] K. Chung, N. Kim, J. Choi, C. Chu, J.-M. Huh, Large-size full color AMOLED TV: advancements and issues, SID Int. Symp. Dig. Tech. Papers 37 (2006) 1958–1963.
[4] T. Gohda, Y. Kobayashi, K. Okano, S. Inoue, K. Okamoto, S. Hashimoto, E. Yamamoto, H. Morita, S. Mitsui, M. Koden, A 3.6-in. 202-ppi full-color AMPLED display fabricated by ink-jet method, SID Int. Symp. Dig. Tech. Papers 37 (2006) 1767–1770.
[5] N.C. van der Vaart, H. Lifka, F.P.M. Budzelaar, J.E.J.M. Rubingh, J.J.L. Hoppenbrouwers, J.F. Dijksman, R.G.F.A. Verbeek, R. van Woudenberg, F.J. Vossen, M.G.H. Hiddink, J.J.W.M. Rosink, T.N.M. Bernards, A. Giraldo, N.D. Young, D.A. Fish, M.J. Childs, W.A. Steer, D. Lee, D.S. George, Towards large-area full-color active-matrix printed polymer OLED television, J. Soc. Inf. Display 13 (2005) 9–16.
[6] T. Hirano, K. Matsuo, K. Kohinata, K. Hanawa, T. Matsumi, E. Matsuda, R. Matsuura, T. Ishibashi, A. Yoshida, T. Sasaoka, Novel laser transfer technology for manufacturing large-sized OLED displays, SID Int. Symp. Dig. Tech. Papers 38 (2007) 1592–1595.
[7] M. Boroson, L. Tutt, K. Nguyen, D. Preuss, M. Culver, G. Phelan, Non-contact OLED color patterning by radiation-induced sublimation transfer (RIST), SID Int. Symp. Dig. Tech. Papers 36 (2005) 972–975.
[8] S. Kim, S. Lee, M. Kim, J. Song, E. Hwang, S. Tamura, S. Kang, H, Kim, C. Kim, J. Lee, J. Kim, S. Cho, J. Cho, M.C. Suh, H. Kim, A 3.0-in. 308-ppi WVGA AMOLED with a top-emission white OLED and color filter, J. Soc. Inf. Display 17 (2009) 145–149.
[9] J.E. Stagnitto, T.W. Palone, C.J. Raes, J.A. White, J. Yokajty, G. Rajeswaran, Method and apparatus for making a shadow mask array, US Patent 6729927, 2004.
[10] T.R. Griffin, T.W. Palone, Aligning OLED substrate to a shadow mask, US Patent 20070184745, 2007.
[11] R.A. Boudreau, R.J. Wilkie, Apparatus and method for registration of shadow masked thin-film patterns, US Patent 4915057, 1990.
[12] P.F. Tian, V. Bulovic, P.E. Burrows, G. Gu, S.R. Forrest, T.X. Zhou, Precise, scalable shadow mask patterning of vacuum-deposited organic light emitting devices, J. Vac. Sci. Technol. A 17 (1999) 2975–2981.
[13] T. Yamada, Electroluminescent display apparatus, US Patent 6366025, 2002.
[14] M.H. Kim, M.W. Song, S.T. Lee, H.D. Kim, J.S. Oh, H.K. Chung, Control of emission zone in a full color AMOLED with a blue common layer, SID Int. Symp. Dig. Tech. Papers 37 (2006) 135–138.
[15] T. Matsumoto, T. Yoshinaga, T. Higo, T. Imai, T. Hirano, T. Sasaoka, High-performance solution-processed OLED enhanced by evaporated common layer, SID Int. Symp. Dig. Tech. Papers 42 (2011) 924–927.
[16] T. Shiga, H. Fujikawa, Y. Taga, Design of multiwavelength resonant cavities for white organic light-emitting diodes, J. Appl. Phys. 93 (2003) 19–22.
[17] S. Han, C. Huang, Z.-H. Lu, Color tunable metal-cavity organic light-emitting diodes with fullerene layer, J. Appl. Phys. 97 (2005) 093102.
[18] S. Chen, G. Tan, W.-Y. Wong, H.-S. Kwok, White organic light-emitting diodes with evenly separated red, green and blue colors for efficiency/color rendition optimization, Adv. Funct. Mater. 21 (2011) 3785–3793.
[19] S. Chen, H.-S. Kwok, Top-emitting white organic light-emitting diodes with a color conversion cap layer, Org. Electron. 12 (2011) 677–681.
[20] J. Lee, J.-I. Lee, J.Y. Lee, H.Y. Chu, Enhanced efficiency and reduced roll-off in blue and white phosphorescent organic light-emitting diodes with a mixed host structure, Appl. Phys. Lett. 94 (2009) 193305.
[21] J.-W. Kang, S.-H. Lee, H.-D. Park, W.-I. Jeong, K.-M. Yoo, Y.-S. Park, J.-J. Kim, Low roll-off of efficiency at high current density in phosphorescent organic light emitting diodes, Appl. Phys. Lett. 90 (2007) 223508.
[22] C.-H. Chang, H.-C. Cheng, Y.-J. Lu, K.-C. Tien, H.-W. Lin, C.-L. Lin, C.-J. Yang, C.-C. Wu, Enhancing color gamut of white OLED displays by using microcavity green pixels, Org. Electron. 11 (2010) 247–254.